Woodchuck Hepatitis Virus Enhancer I and Enhancer II Are Both Involved in N-*myc2* Activation in Woodchuck Liver Tumors

MARC FLAJOLET, PIERRE TIOLLAIS, MARIE-ANNICK BUENDIA, AND GENEVIÈVE FOUREL*

Unité de Recombinaison et Expression Génétique, INSERM U163, Institut Pasteur, 75724 Paris Cedex 15, France

Direct activation of the N-*myc2* oncogene by insertion of woodchuck hepatitis virus (WHV) DNA is a major oncogenic step in woodchuck hepatocarcinogenesis. We previously reported that WHV enhancer II (We2), which controls expression of the core/pregenome RNA, can also activate the N-*myc2* promoter in hepatoma cell lines. To better define the integrated WHV regulatory sequences responsible for N-*myc2* promoter activation in woodchuck liver tumors, we analyzed the structure and enhancer activity of a single viral integrant found at the *win* locus in tumor 2260T1 and mapping approximately 175 kb 3′ of N-*myc2*. This viral insert was made of 11 concatemerized WHV fragments, 5 of which overlapped with We2 sequences and 1 with WHV sequence homologous to that of hepatitis B virus enhancer I (We1). In transient transfection assays in hepatoma-derived cells, the We2 activator was found to be fully effective only when inserted in close proximity to the N-*myc2* promoter whereas the We1 element by itself was apparently devoid of activity. In contrast, the 2260T1 viral insert exhibited a potent enhancer capacity that depended both on multimerized We2 and on We1 sequences. In a survey of different woodchuck hepatomas, both elements were commonly found within integrated viral sequences involved in long-range N-*myc2* activation.

Hepatocellular carcinoma, one of the most frequently occurring human cancers worldwide, is commonly associated with chronic infection by hepatitis B virus (HBV). The incidence of hepatocellular carcinoma is 100-fold higher among HBV carriers than in uninfected populations (2). Two closely related viruses of the hepadnavirus family, woodchuck hepatitis virus (WHV) and ground squirrel hepatitis virus, similarly increase the risk of liver cancer development in their hosts (17, 24) and thus provide suitable model systems. WHV displays an especially strong oncogenic capacity. Virtually all animals infected with WHV at birth succumb to liver cancer within 2 to 4 years, whereas noninfected woodchucks rarely develop spontaneous malignancies over a period of 10 years (20). *cis* activation of *myc* family oncogenes due to the insertion of viral DNA is known to be the key mechanism of woodchuck hepatocarcinogenesis (for reviews, see references 3 and 9). Indeed, a majority of woodchuck liver tumors harbor viral sequences integrated in the immediate vicinity of either c-*myc* or N-*myc* or, more frequently, in N-*myc2* (a functional retroposon) as well as in the *win* locus, which maps 155 to 185 kb downstream of N-*myc2* (10, 11, 14). These viral insertions correlate with activation of transcription from the normal promoter of the target *myc* gene, implying the *cis* action of integrated viral regulatory elements over short as well as long distances. Furthermore, hepatocarcinogenesis is recapitulated in transgenic mice carrying such an altered c-*myc* or N-*myc2* allele (7, 21). The viral regulatory elements involved in the up-regulation of N-*myc2* expression were previously examined by transient transfection assays of different liver cell lines (5, 12, 27, 31). WHV sequences corresponding in position to enhancer I of HBV (We1) appeared devoid of activity on their own. By contrast, sequences corresponding to enhancer II (We2)

strongly activated expression in an orientation-independent but position-dependent manner. We2 activity was shown to result primarily from the synergistic function of one binding site for the liver-enriched HNF1 protein and two sites for the HNF4 protein, although NF-1 and Oct family members were also shown to bind in a central region (12, 28). In those studies, however, WHV's *cis*-activation capacity was dissected through the in vitro-engineered juxtaposition of various portions of the cloned WHV genome with different promoters. To identify WHV regulatory elements genuinely involved in N-*myc2* oncogene activation during hepatocarcinogenesis in the animal, we used another approach, one more relevant to carcinogenesis: analysis of a naturally occurring viral integrant mapping at the *win* locus with regard to its structure and *cis*-activation capacity.

The single integrant from the 2260T1 tumor was preliminarily described in a previous report (11). A library enriched by size selection of *Bgl*II-digested 2260T1 DNA was constructed in the phage vector λ-GEM11 (Promega), and WHV-hybridizing clones were isolated. Restriction mapping of the phage inserts confirmed the insertion of an approximately 3-kb-long WHV sequence in cellular DNA without any additional recombination of the *win* locus, as previously inferred from Southern blot analysis. A 4.3-kb *Sma*I-*Hin*dIII fragment encompassing the viral insertion was further subcloned into the *Sma*I site of the pKS+ vector (Stratagene). The structural organization of the integrated WHV DNA was tentatively determined by restriction mapping and Southern blot hybridization with subgenomic WHV probes. However, it was difficult to recognize any restriction pattern characteristic of the WHV genome, with the exception of the bordering segments (Fig. 1A). The one indicated as the 5′ end corresponded to the region extending from positions 1150 to 1950 on the viral map (with nucleotide numbering as in reference 15), spanning sequences homologous to HBV enhancers I and II, and the 3′ end mapped to the 3′ region of the S gene (positions 400 to 900). Because this initial analysis suggested that there were

* Corresponding author. Present address: CNRS UMR 49, Ecole Normale Supérieure de Lyon, 46 Allée d'Italie, 69634 Lyon Cedex 07, France. Phone: 33-4 72 72 84 53. Fax: 33-4 72 72 86 86. E-mail: Genevieve.Fourel@ens-lyon.fr.
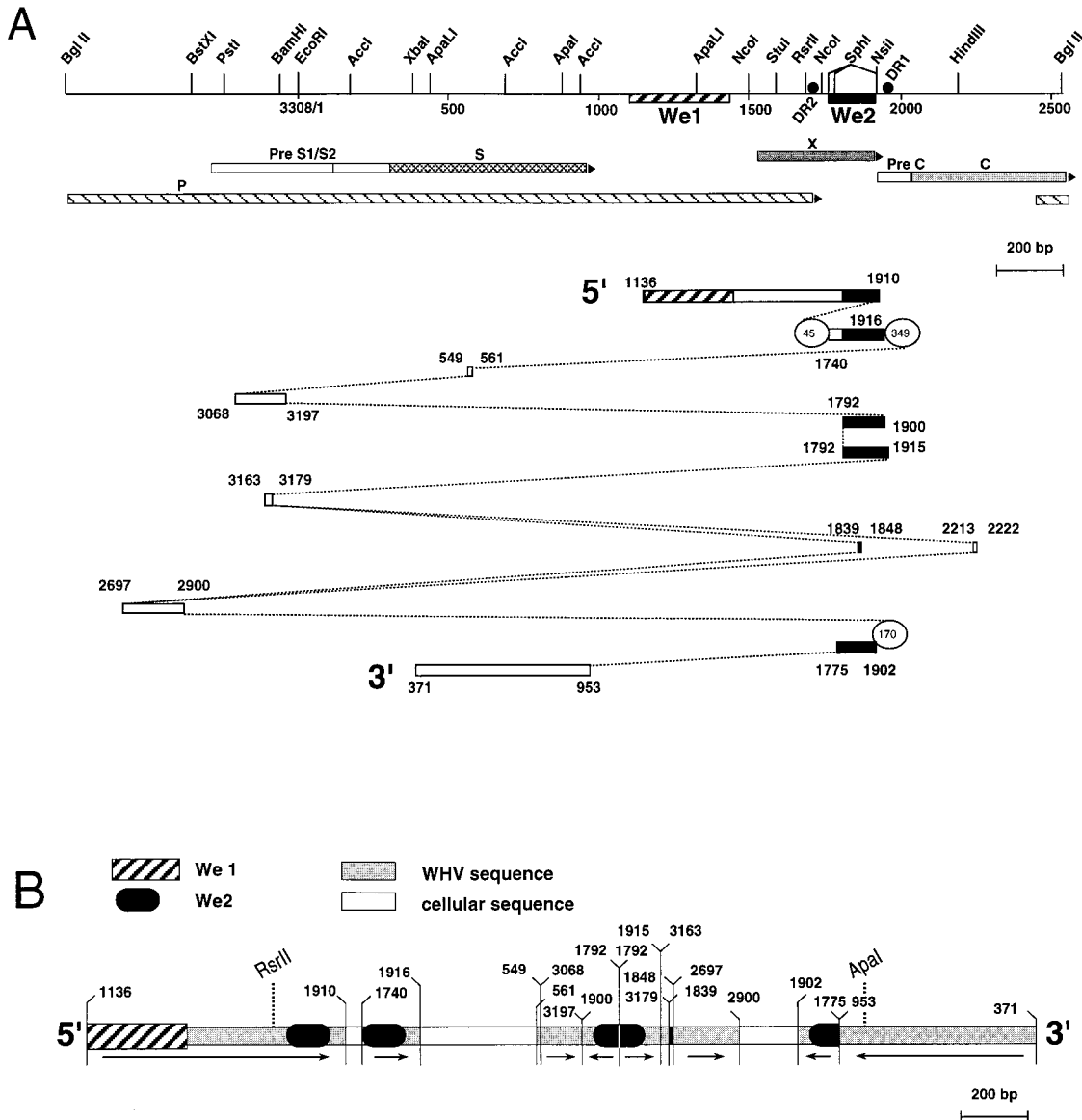
FIG. 1. WHV sequences integrated in the 2260T1 tumor contain We1 and multiple copies of We2. (A) Fragmented representation of the 2260T1 viral integrant. Shown at the top is a physical and genetic map of the WHV genome linearized at the *Bgl*II site, numbered according to reference 15. Restriction sites for enzymes used in the initial mapping of the 2260T1 integrant are indicated. Viral genes are represented as arrows. Hatched box, sequences homologous in position to the HBV enhancer I element (We1) (26); black box, We2 element; closed circles, direct repeats (DR1 and DR2) involved in the replication process. At the bottom is a diagram showing the organization of integrated viral sequences as deduced from sequencing. Viral subgenomic fragments are shown aligned with the corresponding regions of the viral genome. They are represented from top to bottom in an orderly manner indicating their 5′-to-3′ positions within the integrant. Orientations are indicated by the dotted lines and the numbers. For reference, the N-*myc2* gene maps 3′ to the 2260T1 integrant in this representation. The circled numbers represent the lengths (base pairs) of cellular sequences of unknown origin. (B) Linear representation of the 2260T1 viral integrant. The junctions between different viral segments or between viral and cellular fragments are shown by vertical lines, and the numbers indicate the nucleotide positions in the WHV genome. The arrows indicate the direction of transcription along the viral genome. Note that the sequence of nucleotide segment 1839 to 1848 also aligns with positions 2213 to 2222 of the viral genome, as represented in panel A and includes half of an HNF1 binding site (12).

complex rearrangements in the integrated viral DNA, the complete nucleotide sequence of the integrant was determined, revealing concatemerization of 11 subgenomic fragments in either orientation, as represented in Fig. 1. Additional, interposed fragments were probably of cellular origin since they exhibited no similarity to any WHV sequence. An alignment of the subgenomic fragments with the full-length WHV genome is presented in Fig. 1A. Most of the X gene was contained in the 5′ segment, but a C-terminal 33-nucleotide truncation precluded functionality (22), as verified in a transactivation assay

of the simian virus 40 early and N-*myc2* promoters performed as described previously (8) (data not shown). The presence of five copies of the We2 activator element in the central region (coordinates 1740 to 1870 of the WHV genome, as defined in reference 12) was remarkable. Two copies were full-length, while the remaining three were truncated of the external HNF4 binding site (HNF4b [12]). Two segments ending precisely at the same position (nucleotide 1792) were juxtaposed in a back-to-back configuration, gathering two HNF1 and two HNF4 binding sites within a 100-bp region (Fig. 1B). The
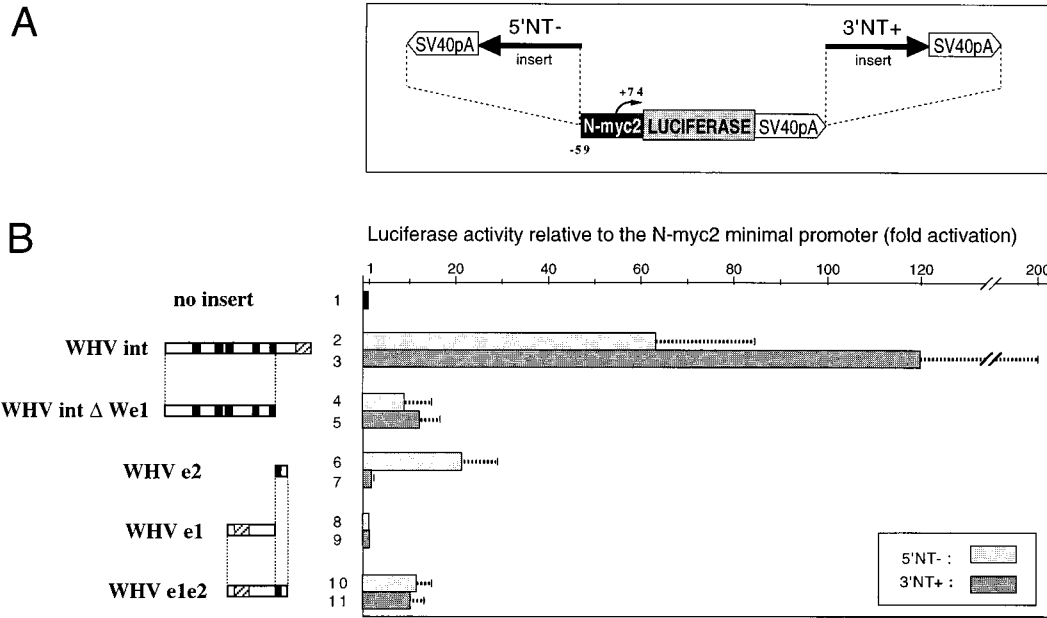
FIG. 2. Enhancer activity of the 2260T1 viral integrant. (A) Schematic representation of the constructs used in transient transfections of HepG2 cells. N-myc2, minimal N-*myc2* promoter (coordinates are relative to the transcription initiation site, indicated by arrows); LUCIFERASE, 5′-truncated firefly luciferase cDNA (4); SV40pA, juxtaposed fragments containing the small intron and the polyadenylation-termination signal of the simian virus 40 genome. N-*myc2* and luciferase ORFs were fused in frame (shaded boxes). Arrows indicate inserted WHV sequences, derived either from the 2260T1 integrant (panel B, lines 2 to 5) or from the wild-type WHV genome (lines 6 to 11). The orientation arbitrarily defined as "+" corresponds to fragments inserted as represented at the left of panel B and to the natural transcriptional orientation for segments directly isolated from the cloned WHV genome (WHV e1, e2, and e1e2). Inserts were placed on either side of the luciferase transcription unit, either 3′ in the plus orientation (3′NT+) or 5′, immediately upstream of the N-*myc2* promoter, in the minus orientation (5′NT−). (B) Plasmids containing the inserts diagrammed on the left, in either the 5′NT− or the 3′NT+ configuration, were transfected into subconfluent HepG2 cells together with a β-galactosidase expression vector. For each construct, luciferase activity was assayed 48 h later and normalized to the β-galactosidase activity. The values shown are relative to those generated by the parent plasmid devoid of the WHV insert. Shown are the averages of data from three experiments. WHVint, 4.3-kb fragment containing the 2260T1 viral integrant; WHVintΔWe1, fragment obtained through truncation of WHVint at an *Rsr*II site; WHVe2, WHVe1, and WHVe1e2, fragments extending from positions 887 to 1501, 1700 to 2103, and 886 to 2103 in the WHV genome, respectively, obtained through restriction digestion of a cloned WHV-8 genome in which the natural unique *Nsi*I site at position 1910 had been displaced to position 2103, where an *Nsi*I site is found in the related virus ground squirrel hepatitis virus.

W2260 woodchuck was experimentally infected at birth with serum containing WHV subtype 7 (WHV-7) (31). Inspection of the sequence at diagnostic positions confirmed the WHV-7 subtype origin of the 2260T1 viral integrant.

Transcription of integrated hepadnavirus sequences from the strong preS2/S promoter has been previously observed in a number of woodchuck and human liver tumors (25, 30) and can lead to the synthesis of a potentially oncogenic, truncated PreS2/S protein (16). However, this promoter (18) was not represented in the 2260T1 viral integrant. Northern blot analysis of RNA extracted from a 2260T1 liver tumor with a WHV probe did not detect any viral transcript (data not shown), in spite of the presence of multiple copies of the C promoter and one copy of the X promoter. Thus, the 2260T1 viral integrant does not appear to be expressed. Examination of the cellular genomic DNA flanking the 2260T1 viral insert in the 4.3-kb fragment analyzed failed to reveal any potential coding regions (data not shown). In addition, running the XGRAIL program on a larger, 17-kb sequenced region of the *win* locus similarly did not conclusively identify any exon (10). Thus, the 2260T1 viral insert does not appear to exert oncogenic potential through either the production of a viral transactivator or the local *cis* activation of an oncogene. Since the N-*myc2* gene is expressed at a very high level in the 2260T1 tumor (11), and since a high density of regulatory elements was evidenced in the viral insert, we investigated the capacity of the 2260T1 integrant to *cis* activate the N-*myc2* promoter.

Luciferase constructs containing either the 4.3-kb *Sma*I-*Hin*dIII 2260T1 fragment or control WHV subgenomic fragments were generated and transiently transfected in the HepG2 human liver cell line as described previously (12). Insertion of an N-*myc2* promoter-luciferase fragment in either orientation next to the viral sequences resulted in constructs carrying a viral insert either in a proximal position relative to the N-*myc2* promoter or in a distal position, outside of the transcription unit (Fig. 2A). The 2260T1 viral insert proved to be able to potently activate the N-*myc2* promoter when inserted in a distal or in a 5′-proximal position (Fig. 2B, lines 2 and 3), leading on average to 100-fold-induced expression levels in HepG2 cells. As mentioned above, the partial X open reading frame (ORF) found in the insert was nonfunctional and thus did not contribute to this effect. The strong enhancer activity of the 2260T1 integrant contrasts with properties of the isolated We2 element, which is significantly active only when inserted in close proximity to the promoter (Fig. 2B, lines 6 and 7) (12). The 2260T1 viral insert therefore exhibits bona fide enhancer properties and is a potent activator of the N-*myc2* promoter.

Further deletion mapping of the 2260T1 viral insert was carried out to identify sequences involved in transcriptional activation. Deletion of S gene sequences downstream of the *Apa*I site (Fig. 1B, 3′ end) did not affect the *cis*-activation properties of the insert (data not shown). In contrast, deletion of sequences upstream of the *Rsr*II site (Fig. 1B, 5′ end) severely impaired the activation in the WHVintΔWe1 construct (Fig. 2B, lines 4 and 5). A position-independent, enhancer-like

effect was still observed, suggesting that long-range transcription-activating properties can be conferred on We2 through multimerization. Furthermore, sequences encompassed between positions 1136 and 1700 exhibit a striking amplification effect on the activity of the WHVintΔWe1 fragment. Sequences corresponding in position to HBV enhancer I and called We1 are contained within this segment. Although some patches of nucleotide homology between the WHV and HBV sequences overlap with known binding sites for different transcription factors (5), We1 sequences by themselves did not exhibit any capacity to activate the minimal N-*myc2* promoter (Fig. 2B, lines 8 and 9). Similar data from studies using N-*myc2* promoter sequences extending up to position −1100 (12, 27) as well as other promoters (5) were previously reported. This apparent lack of activity was previously attributed to relative deficiency, inherent in liver-derived cell lines, in WHV expression compared to HBV expression (5). However, in our transient transfection assays, provision of both We1 and We2 sequences within a contiguous subgenomic fragment yielded a genuine enhancer effect, as efficient in a 5′ configuration as in a 3′ configuration (Fig. 2B, lines 10 and 11) and reaching levels close to those of the WHVintΔWe1 construct. Although the X ORF is also included within this WHV fragment, previous investigations demonstrated that the contribution of X trans-activation to the apparent *cis*-activation effect was not significant (12, 27). Thus, although inactive in direct *cis* activation on its own, the We1 element was shown here to potentiate the activity of We2, either in a single-copy construct by conferring long-range activation properties or in a naturally occurring viral insertion by amplifying the enhancer effect of multiple, concatemerized We2 copies. This peculiar form of cooperativity between We1 and We2 is reminiscent of the reported synergy between enhancers I and II of HBV (23). It is also analogous to previously described properties of the RFX binding site found within HBV enhancer I, a crucial enhancer element that acts only via interaction with a second enhancer element exhibiting a genuine transcriptional activation capacity (6). Further studies are needed to address whether the amplifier property of We1 is specific to We2 or it can affect other transcriptional activator elements.

To investigate the enhancer capacity of the 2260T1 viral integrant over large distances, constructs that carry artificially abutted N-*myc2* genes and portions of the *win* locus, derived either from the rearranged allele of tumor 2260T1 or from a wild-type allele, were generated (Fig. 3A, constructs *b*, *c*, and *d*). Plasmids containing only the N-*myc2* gene (construct *a*), N-*myc2* ligated to the same 4.3-kb viral-integrant-encompassing fragment as that inserted in the WHVint luciferase construct (construct *e*), or random 16-kb woodchuck genomic DNA fragments (constructs *f*, *g*, and *h*) were also created as controls. After transient transfection of HepG2 cells, the production of faithfully initiated N-*myc2* transcripts was assessed by RNase mapping with a probe encompassing the N-*myc2* transcription start site (13) (Fig. 3B). An RNA sample isolated from an N-*myc2*-expressing woodchuck liver tumor and a 1/10 dilution thereof were analyzed in parallel as controls. Similar levels of N-*myc2* RNA were observed on transfection of constructs *d* and *e*, and these levels were much higher than those produced from construct *a* (Fig. 3B, compare lanes 3 and 4, 9 and 10, and 11 and 12). In construct *d*, viral sequences are separated from the N-*myc2* promoter by 13 kb of *win* sequence in one direction and by 7 kb of DNA in the other direction due to the circular nature of the transfected plasmids. These results suggest that the 2260T1 viral integrant enhances N-*myc2* expression from a distance as well as it does when inserted in close proximity to the promoter.
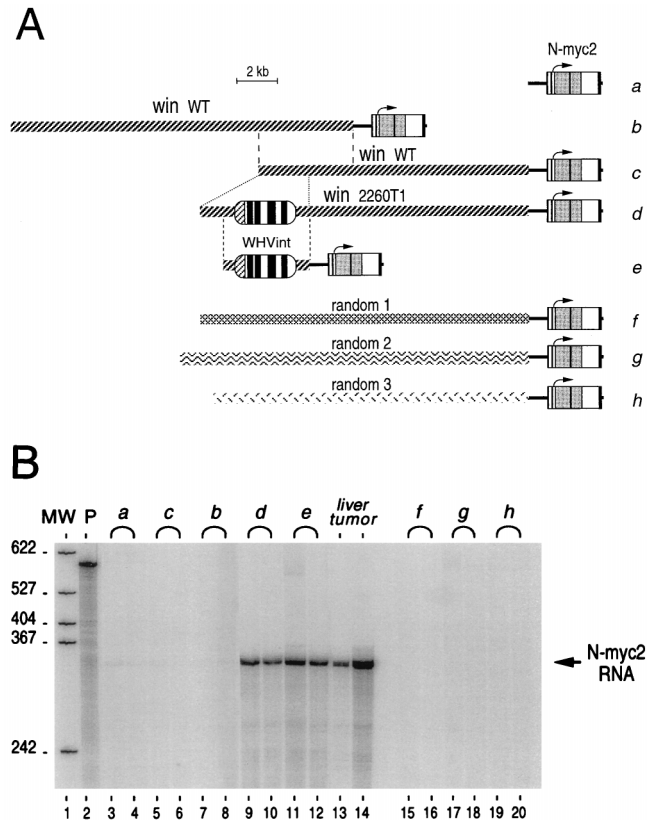

FIG. 3. Enhancer activity of the 2260T1 viral integrant over large distances and absence of intrinsic regulatory activity for the *win* locus in transient transfection. (A) Schematic representations of the constructs used in transient transfections of HepG2 cells. The DNA fragments represented were inserted in pBluescript KS+ (Stratagene). For construct *a*, the 3.2-kb *Hin*dIII insert containing the N-*myc2* gene is represented as a thick black line, with the region showing homology to N-*myc* exons designated by an open box and the N-*myc2* ORF designated by a shaded box. This fragment includes all the regulatory elements of N-*myc2* identified to date (13). It is present as a *Not*I insert in each construct, only the additional sequences of which will be described subsequently. Construct *b* is a 16.7-kb region of the wild-type (WT) *win* locus encompassing the majority of characterized WHV integration sites in *win* (10). It is the insert from a phage isolated from the 134TA genomic library (11) and is derived from the unrearranged *win* allele as confirmed by the independent isolation of overlapping clones from different libraries (10). Construct *c* is a 13.2-kb *Bgl*II fragment of the wild-type *win* locus, isolated from phage λ134TA.1 (11); constructs *b* and *c* overlap in a 4.7-kb region containing the WHV integration site of tumor 2260T1. Construct *d* consists of the same region of *win* as that in construct *c* but was isolated from a rearranged allele of tumor 2260T1 and thus contains the viral integrant (16.15 kb) (11). Construct *e* carries the same insert as the luciferase construct WHVint, a 4.3-kb *Sma*I-*Hin*dIII fragment excised from insert *d*. For constructs *f*, *g*, and *h*, a random population of phages from the 134TA genomic library was grown and their inserts were isolated and subcloned. Three clones which do not contain any *Not*I restriction sites were randomly chosen, and these inserts could thus be assumed to represent random woodchuck genomic sequence. They are approximately 16 kb long. Details of the construction strategies are available upon request. (B) Constructs were transiently transfected in subconfluent HepG2 cells together with a β-galactosidase expression vector, and total RNA were prepared as described previously (12). RNAs were analyzed by RNase mapping, using a probe encompassing the N-*myc2* transcription start site and RNase T2 as described previously (12, 13). Normalization of the input quantity was done taking into account the corresponding β-galactosidase activity. Variations in transfection efficiency did not exceed twofold. Lanes: MW, molecular size markers (in nucleotides); P, N-*myc2* antisense RNA probe, unprocessed; a to h, transfected constructs, as indicated at the right of panel A (preparative transfections were performed in duplicate, and the corresponding RNase mapping products were run in consecutive lanes); liver tumor, 0.1 μg (lane 13) or 1 μg (lane 14) of RNA prepared from an N-*myc2*-expressing woodchuck liver tumor. Faint signals corresponding to faithfully initiated N-*myc2* transcripts, visible in lanes 3, 4, 19, and 20, were more readily detected after longer exposures.
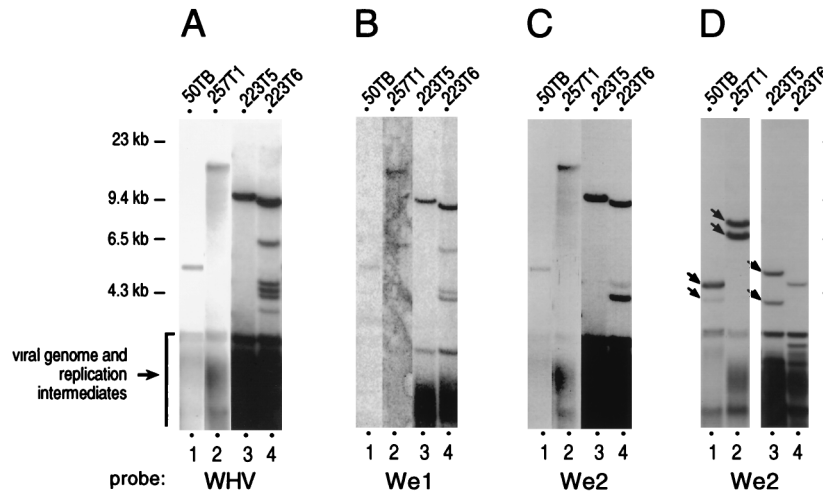
FIG. 4. Single viral integrants at the *win* locus in woodchuck liver tumors contain We1 and multiple copies of We2. Southern blot analysis of genomic DNA from tumors 50TB, 257T1, 223T5, and 223T6 was performed as described previously (11). The 50TB, 257T1, and 223T5 tumors each contain a single viral integrant inserted at the *win* locus. The 223T6 tumor, which harbors multiple viral integrations displaying differential hybridization with the probes used here, is shown as a hybridization control. Genomic DNA was digested with *Pvu*II (panels A to C), *Hin*dIII (panel D, lanes 1 and 2), or *Xba*I (panel D, lanes 3 and 4). The probes used for hybridization are indicated below the panels. The full-length WHV probe (A) and the We1 probe (positions 1178 to 1478) (B) were obtained by random priming with the cloned WHV-8 genome as a template. The We2 template for random priming (positions 1700 to 1910) (C and D) was generated by self-ligation of a WHV nucleotide 1700 to 1910 PCR fragment with *Bam*HI and *Bgl*II cohesive ends, digestion by *Bam*HI and *Bgl*II to rehydrolyze head-to-head ligations, and purification of trimeric structures. Probe stripping for sequential hybridization was achieved through two 15-min incubations of the Hybond-N+ membrane (Amersham) in 0.4 N NaOH at room temperature followed by two 15-min neutralizations in 50 mM sodium phosphate buffer, pH 6.5. Complete elimination of the signal was verified by using a PhosphorImager (Molecular Dynamics). The positions of size markers and of WHV genome and replicative intermediates are indicated.

In contrast, RNAs derived from each of the other constructs were either barely detectable (Fig. 3B, lanes 3, 4, 19, and 20) or could not be detected at all (lanes 5 to 8 and 15 to 18). In this assay, the *win* locus does not behave differently from two randomly chosen woodchuck genomic loci and thus does not seem endowed with transcriptional regulatory properties. The possibility that small plasmids might transfect more effectively than large ones could account for the fact that N-*myc2* transcripts are detected on transfection of construct *a* but not of constructs *b*, *c*, *f*, and *g*. Alternatively, including large genomic DNA fragments in plasmids might facilitate the assembly of a chromatin-like structure and lead to gene repression in transient transfections. In this hypothesis, part of the mechanism of N-*myc2* activation by viral sequences in construct *d* would consist of antirepression, and the faint signal associated with control construct *h* might also be accounted for by specific alleviation of such a repression phenomenon.

Collectively, these results support a model in which sequences of the wild-type *win* locus are neutral with respect to N-*myc2* transcriptional regulation. Viral sequences might be found preferentially integrated at the *win* locus in woodchuck liver tumors either due to increased local accessibility or because the high-order chromatin organization of the chromosomal domain facilitates interaction between integrated viral enhancers and the N-*myc2* promoter over a 155- to 185-kb distance.

Additional viral sequences integrated into the *win* locus in woodchuck liver tumors were further analyzed by Southern blotting with subgenomic WHV probes. Preliminary characterizations (11) allowed the selection of three woodchuck liver tumors (50TB, 257T1, and 223T5) from a panel of 56 samples by the following two criteria: (i) they displayed a single viral integrant, as revealed by detection of a single high-molecular-weight band hybridizing to a full-length WHV probe in tumor DNA digested with *Pvu*II (an enzyme that does not cut in the

viral genome) (Fig. 4A, lanes 1 to 3); and (ii) the viral integrants mapped at the *win* locus without major rearrangement of the surrounding cellular DNA (10, 11). Each of these three viral integrants was revealed by both We1 and We2 probes, which span regions 1158 to 1478 and 1700 to 1910 of the viral genome, respectively (Fig. 4B and C, lanes 1 to 3). A tumor DNA harboring at least five integrants displaying differential hybridization with either probe was loaded in lanes 4 as a specificity control. Furthermore, digestion of tumor DNA with restriction enzymes that cut once in the WHV genome but not in the nucleotide 1700 to 1910 fragment (*Hin*dIII, *Nsi*I, or *Xba*I) yielded at least two We2-hybridizing fragments in each case (Fig. 4D, lanes 1 to 3, and data not shown). Thus, at least two copies of the We2 element were present in each of the three integrants analyzed. These data suggest that multimerization of We2, which can produce a potent enhancer effect, may be commonly encountered in viral sequences integrated at the *win* locus. These cases are reminiscent of rearrangements with internal duplications of various lengths in retroviral long terminal repeats of proviruses isolated from tumors induced by weakly pathogenic retroviruses. These structures exhibit enhancer activity, in contrast to the corresponding wild-type long-terminal repeats, and they appear to be selected during tumorigenesis owing to their direct involvement in oncogene *cis* activation (1, 19).

We previously described the presence of We1 and/or We2 sequences in a large majority of WHV-integrated sequences (31), and about 25% of the viral integrations involved in N-*myc2* activation overlap with either We1 or We2 sequences in an exclusive fashion (10). The data presented here lend further support to the existence of two independent regulatory elements in WHV that can trigger N-*myc2* transcription at the roots of the hepatocarcinogenesis process. We2, which overlaps with sequences upstream of the WHV C promoter, was recently characterized as a strong, positively acting regulatory element that nonetheless exhibits a minimal enhancer capacity

on the N-*myc2* promoter (12, 27). Here we have shown that We2 can naturally acquire distance-independent properties upon multimerization in the integrated state. We1 sequences, whose role remains elusive so far, are seemingly able to amplify the activity of adjacent transcriptional activator elements. It is conceivable that We1 synergizes with genuine or cryptic cellular activator elements lying in the vicinity of the viral integrant to activate the N-*myc2* promoter independently of We2. Two alternative mechanisms can be envisioned to account for the amplifier function of We1. We1 may somehow stabilize physical interactions between factors bound within the activator element and at the N-*myc2* promoter; alternatively, We1 may alleviate a negative control imposed on the N-*myc2* promoter and confer permissiveness to direct transcriptional activation as recently reported for other enhancers (29). We do not formally exclude the possibility that We1 is additionally endowed with more-classical transcriptional activation properties that were deficient in the reported experimental contexts (5, 12, 27) but might be detected in a more physiological system which remains to be elaborated. However, our study provides a preliminary framework for future dissection of the We1 sequences in order to identify factors responsible for the described amplifier activity of We1. The combination of multimerized We2 sequences with We1 observed in four viral integrants at the *win* locus can generate impressive enhancer effects. Expression levels from the N-*myc2* promoter thereby activated can be further increased on cooperation of *trans*-acting pathways (8), and both mechanisms might synergize in stimulating oncogene transcription in woodchuck livers chronically infected with WHV.

REFERENCES

1. **Athas, G. B., P. Lobelle-Rich, and L. S. Levy.** 1995. Function of a unique sequence motif in the long terminal repeat of feline leukemia virus isolated from an unusual set of naturally occurring tumors. J. Virol. **69:**3324–3332.
2. **Beasley, R. P., C. C. Lin, L. Y. Hwang, and C. S. Chien.** 1981. Hepatocellular carcinoma and hepatitis B virus: a prospective study of 22,707 men in Taiwan. Lancet **ii:**1129–1133.
3. **Buendia, M. A.** 1994. Animal models for hepatitis B virus and liver cancer, p. 211–224. *In* C. Bréchot (ed.), Primary liver cancer: etiological and progression factors. CRC Press, Boca Raton, Fla.
4. **de Wet, J. R., K. V. Wood, M. DeLuca, D. R. Helinski, and S. Subramani.** 1987. Firefly luciferase gene: structure and expression in mammalian cells. Mol. Cell. Biol. **7:**725–737.
5. **Di, Q., J. Summers, J. B. Burch, and W. S. Mason.** 1997. Major differences between WHV and HBV in the regulation of transcription. Virology **229:** 25–35.
6. **Dikstein, R., O. Faktor, R. Ben-Levy, and Y. Shaul.** 1990. Functional organization of the hepatitis B virus enhancer. Mol. Cell. Biol. **10:**3683–3689.
7. **Etiemble, J., C. Degott, C. A. Renard, G. Fourel, B. Shamoon, L. Vitviski-Trépo, T. Y. Hsu, P. Tiollais, and M. A. Buendia.** 1994. Liver-specific expression and high oncogenic efficiency of a c-*myc* transgene activated by woodchuck hepatitis virus insertion. Oncogene **9:**727–737.
8. **Flajolet, M., A. Gegonne, J. Ghysdael, P. Tiollais, M.-A. Buendia, and G. Fourel.** 1997. Cellular and viral trans-acting factors modulate N-*myc2* promoter activity in woodchuck liver tumors. Oncogene **15:**1103–1110.
9. **Fourel, G.** 1994. Genetic and epigenetic alterations of gene expression in the course of hepatocarcinogenesis, p. 297–343. *In* F. Tronche and M. Yaniv (ed.), Liver gene expression. R. G. Landes Company, Austin, Tex.
10. **Fourel, G.** Unpublished data.
11. **Fourel, G., J. Couturier, Y. Wei, F. Apiou, P. Tiollais, and M. A. Buendia.** 1994. Evidence for long-range oncogene activation by hepadnavirus insertion. EMBO J. **13:**2526–2534.
12. **Fourel, G., F. Ringeisen, M. Flajolet, F. Tronche, M. Pontoglio, P. Tiollais, and M.-A. Buendia.** 1996. The HNF1/HNF4-dependent We2 element of woodchuck hepatitis virus controls viral replication and can activate the N-*myc2* promoter. J. Virol. **70:**8571–8583.
13. **Fourel, G., C. Transy, B. C. Tennant, and M. A. Buendia.** 1992. Expression of the woodchuck N-*myc2* retroposon in brain and in liver tumors is driven by a cryptic N-*myc* promoter. Mol. Cell. Biol. **12:**5336–5344.
14. **Fourel, G., C. Trépo, L. Bougueleret, B. Henglein, A. Ponzetto, P. Tiollais, and M. A. Buendia.** 1990. Frequent activation of N-*myc* genes by hepadnavirus insertion in woodchuck liver tumours. Nature **347:**294–298.
15. **Galibert, F., T. N. Chen, and E. Mandart.** 1982. Nucleotide sequence of a cloned woodchuck hepatitis virus genome: comparison with the hepatitis B virus sequence. J. Virol. **41:**51–65.
16. **Kekulé, A. S., U. Lauer, M. Meyer, W. H. Caselmann, P. H. Hofschneider, and R. Koshy.** 1990. The pre-S2/S region of integrated hepatitis B virus DNA encodes a transcriptional transactivator. Nature **343:**457–461.
17. **Marion, P. L., M. J. Van Davelaar, S. S. Knight, F. H. Salazar, G. Garcia, H. Popper, and W. S. Robinson.** 1986. Hepatocellular carcinoma in ground squirrels persistently infected with ground squirrel hepatitis virus. Proc. Natl. Acad. Sci. USA **83:**4543–4546.
18. **Möröy, T., J. Etiemble, C. Trépo, P. Tiollais, and M. A. Buendia.** 1985. Transcription of woodchuck hepatitis virus in the chronically infected liver. EMBO J. **4:**1507–1514.
19. **Morrison, H. L., B. Soni, and J. Lenz.** 1995. Long terminal repeat enhancer core sequences in proviruses adjacent to c-*myc* in T-cell lymphomas induced by a murine retrovirus. J. Virol. **69:**446–455.
20. **Popper, H., L. Roth, R. H. Purcell, B. C. Tennant, and J. L. Gerin.** 1987. Hepatocarcinogenicity of the woodchuck hepatitis virus. Proc. Natl. Acad. Sci. USA **84:**866–870.
21. **Renard, C.-A., G. Fourel, and M.-A. Buendia.** Unpublished data.
22. **Runkel, L., M. Fischer, and H. Schaller.** 1993. Two-codon insertion mutations of the HBx define two separate regions necessary for its trans-activation function. Virology **197:**529–536.
23. **Su, H., and J. K. Yee.** 1992. Regulation of hepatitis B virus gene expression by its two enhancers. Proc. Natl. Acad. Sci. USA **89:**2708–2712.
24. **Summers, J., J. M. Smolec, and R. Snyder.** 1978. A virus similar to human hepatitis B virus associated with hepatitis and hepatoma in woodchucks. Proc. Natl. Acad. Sci. USA **75:**4533–4537.
25. **Terris, B., A. Marchio, M.-G. Mattei, E. Fagan, A. Lol, P. Tiollais, and A. Dejean.** 1992. Expression anormale de séquences du virus de l'hépatite B intégrées dans des carcinomes hépatocellulaires humains. Gastroenterol. Clin. Biol. **16:**511–517.
26. **Trujillo, M. A., J. Letrovsky, H. F. Maguire, M. Lopez-Cabrera, and A. Siddiqui.** 1991. Functional analysis of a liver-specific enhancer of the hepatitis B virus. Proc. Natl. Acad. Sci. USA **88:**3797–3801.
27. **Ueda, K., Y. Wei, and D. Ganem.** 1996. Activation of N-*myc2* gene expression by cis-acting elements of oncogenic hepadnaviral genomes: key role of enhancer II. Virology **217:**413–417.
28. **Ueda, K., Y. Wei, and D. Ganem.** 1996. Cellular factors controlling the activity of woodchuck hepatitis virus enhancer II. J. Virol. **70:**4714–4723.
29. **Walters, M. C., W. Magis, S. Fiering, J. Eidemiller, D. Scalzo, M. Groudine, and D. I. K. Martin.** 1996. Transcriptional enhancers act in *cis* to suppress position-effect variegation. Genes Dev. **10:**185–195.
30. **Wei, Y., J. Etiemble, C. A. Renard, P. Tiollais, and M.-A. Buendia.** 1996. Unusual activation of the integrated preS1 promoter of woodchuck hepatitis virus in a liver tumor. J. Gen. Virol. **77:**177–182.
31. **Wei, Y., G. Fourel, A. Ponzetto, M. Silvestro, P. Tiollais, and M.-A. Buendia.** 1992. Hepadnavirus integration: mechanisms of activation of the N-*myc2* retrotransposon in woodchuck liver tumors. J. Virol. **66:**5265–5276.